Oil Shale, 2018, Vol. 35, No. 3, pp. 214–229
doi: https://doi.org/10.3176/oil.2018.3.02
ISSN 0208-189X

EXPERIMENTAL RESEARCH OF THE PYROLYTIC PROPERTIES AND MINERAL COMPONENTS OF BOGDA OIL SHALE, CHINA

HONGGE ZHANG[(a)*], JIAN LIU[(a)], ZHIQIN KANG[(b)], DONG YANG[(b)]

[(a)] College of Mining Engineering, Taiyuan University of Technology, Taiyuan 030024, China
[(b)] Mining Technology Institute, Taiyuan University of Technology, Taiyuan 030024, China

Abstract. *The purpose of this paper was to investigate the pyrolysis properties and mineral structures of Bogda oil shale, Xinjiang, China. To this end, techniques such as Fourier transform infrared spectroscopy (FTIR), X-ray diffraction (XRD), scanning electron microscopy (SEM), energy dispersive spectrometry (EDS) and thermogravimetry-mass spectrometry (TG-MS) were used. The results showed that oil shale was rich in clay minerals, quartz, calcite, frondelite and pyrite. Aliphatic hydrocarbons were mainly dominant in the functional groups contained in the organic material of oil shale whose semi-coke possessed diverse structures of polycyclic aromatic hydrocarbons. The pyrolysis process of Bogda oil shale was conducted in three stages: from room temperature to 320 °C, 320 °C to 630 °C, and 630 °C to 800 °C. The pyrolysis was the most intensive in the temperature range of 320–630 °C. The mass loss of oil shale in this temperature range accounted for 70% of the total mass loss. The volatile materials were pyrolysed rapidly. The main gaseous pyrolysis products included H_2O, CO_2, H_2, CH_4, and some lower alkanes.*

Keywords: *oil shale pyrolysis, microstructure, Fourier transform infrared spectroscopy, X-ray diffraction, Bogda oil shale.*

1. Introduction

Abundant reserves of oil shale resources are an important supplement to fossil fuel resources with huge development and utilization potential. Among fossil energy sources, the heat quantity of converted oil shale ranks second after coal [1, 2]. The H/C atomic ratio of oil shale as a fossil fuel is higher

* Corresponding author: e-mail *dove1106@163.com*

than that of organic matter in coal. In addition, the amount of oil produced by the pyrolysis of oil shale is also higher than that from the pyrolysis of coal containing the same mass of organic matter [3, 4]. Although oil shale has a high ash content, refined shale oil is an excellent fluid fuel and chemical material and can be used as an alternative to oil [5]. The characteristics of oil shale have been influenced by many factors, including geological conditions, formation age, and the degree of metamorphism of the organic matter therein. The structural morphology of minerals and organic matter in oil shale undergo significant changes, which significantly affect the pyrolytic processing of oil shale and the corresponding products [6–8]. Oil shale is mainly composed of two parts: organic and inorganic. The mineral composition is relatively complex and usually includes clay minerals (kaolinite, montmorillonite, illite), carbonates (dolomite, calcite), quartz, pyrite, etc. At present, the development and utilization of oil shale mainly focuses on the following aspects: distillation to produce shale oil, combustion to generate electricity, gasification, and ash utilization [9, 10]. The pyrolytic properties and mineral structures of oil shale influence its utilization efficiency [11]. Sadiki et al. [12] reported that the optimum pyrolysis temperature of Morocco oil shale was 520–630 °C, and a large quantity of low-sulfur shale oil could be obtained in this range. Yu and Jiang [13] stated that the pyrolysis of Chinese Huadian oil shale could be divided into two temperature steps and that increasing the heating rate was useful to improve the pyrolysis yield. Li and Yue [14] found that C–O and C–S in oil shale were easily oxidized at the low-temperature stage of pyrolysis. Allred [15] obtained the activation energy of oil shale pyrolysis at different heating rates via a first-order kinetic equation. He established that the higher the activation energy, the higher the amount of heat required for the pyrolysis reaction. Nazzal [16] studied the pyrolysis of oil shale of different particle sizes. He claimed that oil shale with large particle size produced more hydrocarbon gas during the pyrolysis process compared with oil shale of smaller particle size. The retorting technique of lump oil shale serves as a basis for the overall utilization of oil shale. Hence, having better knowledge about the pyrolytic properties of oil shale is of significance to its further processing. The Xinjiang Uighur Autonomous Region in Northwest China is abundant in rich oil shale resources: the reserves in the southeast margin of the Junggar Basin amount to 54.8 billion tons, while the Bogda region with its expected reserves of more than 5 billion tons represents a characteristic oil shale area. In this research, Fourier transform infrared spectroscopy (FTIR), X-ray diffraction (XRD), thermogravimetry-mass spectrometry (TG-MS), scanning electron microscopy (SEM) and energy dispersive spectrometry (EDS) were used to analyse the pyrolytic properties of Bogda oil shale and characterize its pyrolysis products.

2. Experiments

2.1. Pyrolysis

The oil shale specimens used for pyrolysis were ground and screened to a particle size of less than 0.2 mm. The oil content and gas production of the specimens were measured to be 6.96% and 3.71%, respectively. The results of industrial and composition analysis of oil shale are presented in Table 1. The pyrolysis experiment was performed in a tubular furnace. The oil shale specimens were put into a quartz reactor and then heated to 200, 400, 600, 800 and 1000 °C at a heating rate of 10 °C/min. Afterward the specimens were held at the respective temperatures for 60 minutes and then cooled to room temperature before use.

Table 1. Technical parameters of Bogda oil shale

Density, g/cm^3	Oil content, %	Char yield, %	Moisture, %	Volatile, %	Ash, %	Fixed carbon, %	Calorific value, MJ/kg
2.20	11.08	68.45	4.31	35.18	53.27	7.11	6.88

2.2. Fourier transform infrared spectroscopy

For infrared spectrum measurements, a Nicolet IS10 FTIR Spectrometer with a spectral resolution of 4 cm^{-1} was used. Before testing, 1 mg specimens and 200 mg KBr were ground after mixing. Then the specimens were continuously compressed for 2 minutes into sheets under a confining pressure of 10 MPa and dried for 48 h in a vacuum dryer to reduce the influence of water on the experimental results.

2.3. Thermogravimetry-mass spectrometry

The TG-MS testing was carried out on a 204HP Phoenix thermal analyser (Netzsch Group, Germany) from room temperature to 800 °C. The experiments were performed at heating rates of 10, 20 and 30 °C/min with a nitrogen gas flow of 100 ml/min. For analysis of gaseous pyrolysis products an Omnistar™/Thermostar on-line mass spectrometer with a mass number of 1 to 200 was used.

2.4. X-ray diffraction

For the XRD testing a Shimadzu XRD-7000 diffractometer (Japan) was employed. In the experiments, the Kul wire was used as the copper target, with a tube voltage of 40.0 kV, a tube current of 30.0 mA, a receiving slit of 0.3 mm width, a scanning rate of 8.00 °/min, a beam spread of 0.02°, and a step-scan time of 0.20 s. The scanning range was $5.00° \leq 2\theta \leq 85.00°$ run in continuous scanning mode.

2.5. Scanning electron microscopy and energy dispersive spectrometry

For the SEM experiment a specimen of 2 cm in diameter was used. The test instrument was the Inspect S50 scanning electron microscope (FEI, US) with 500× magnification. The EDS test was conducted employing the Bruker EDS QUANTAX energy dispersive spectrometer (Germany). The electron beam diameter was 5–10 cm, and the hot electron flow intensity was 20 keV.

3. Results and discussion

3.1. Pyrolysis process and products

Figure 1 shows the TG curves of mass loss of Bogda oil shale samples heated during pyrolysis at different rates. At the same time, the samples underwent physical changes, such as the softening and recombination of

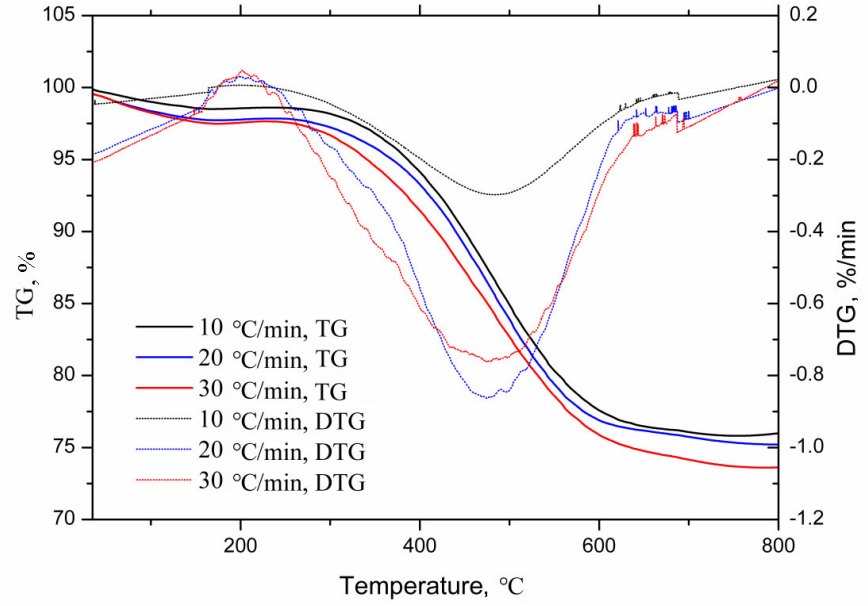

Fig. 1. TG/DTG curves of Bogda oil shale samples at different heating rates.

minerals, before production of tar. Moreover, some gases produced from the pyrolysis of certain minerals also led to mass loss. The oil shale specimens experienced the mass loss in the low-temperature region from room temperature to 320 °C, due to the evaporation of water within them, and of interlayer water in their clay minerals. The oil shale mass loss in the low-temperature zone was mainly caused by the precipitation of water in it, while the mass loss from 320 to 630 °C mainly resulted from the pyrolysis of hydrocarbons. Within this temperature range, the pyrolysis of volatile matter mostly occurred, causing a significant decline of TG curves. The pyrolysis of oil shale usually involves its decomposition into oil and gas, and semi-coking products in two steps. In this work, oil shale was first pyrolysed into tar, which was then further pyrolysed to obtain the final products of pyrolysis. The real mechanism underpinning the pyrolysis of oil shale was quite complex. It involved multiple serial and parallel reactions. Above 630 °C, the TG curve exhibited a continued mass loss. The TG curve was relatively smooth, and the pyrolysis of carbonates, including calcite, dolomite and abundant ankerite, chiefly occurred at temperatures higher than 630 °C.

Figure 2 shows the MS curves for the gaseous product arising during the pyrolysis process. H_2 mainly emitted from the degradation of the hydrogen-rich substrate and the polycondensation of pyrolysed free radicals. At temperatures above 600 °C, H_2 resulted from the decomposition of coagulated aromatic matter, coagulated aromatic structures and heterocyclic compounds. The peaks appearing at temperatures below 200 °C were assignable to the exterior water of the specimens. Large amounts of H_2O were produced by the decomposition of various oxygen components; the phenolic hydroxyl was chemically combined with water molecules present in oil shale. Moreover, at 600 °C, small amounts of H_2O were generated by the decomposition of oxygen components of higher heat resistance, such as heterocyclic aromatic compounds. At a temperature of approximately 600 °C, there appeared a strong peak that belonged to CO_2 produced by the decomposition of aliphatic and aromatic carboxyl groups in oil shale. As the temperature rose, more stable ether structures and carbonyl functional groups in the samples were fractured. Among the fractured groups, some were bonded with oxygen atoms to further generate CO_2. At lower temperatures, CH_4 was produced due to the rupture of the aliphatic bond of long-chain C–C structures, while at higher temperatures, its release likely resulted from the rupture of the bonds between aromatic methyl groups or aralkyl groups. Furthermore, it was found that maximum amounts of alkane components, such as C_2H_4, C_2H_6 and C_3H_8, were generated at temperatures between 300 and 600 °C. This finding agreed with TG test results.

(a)

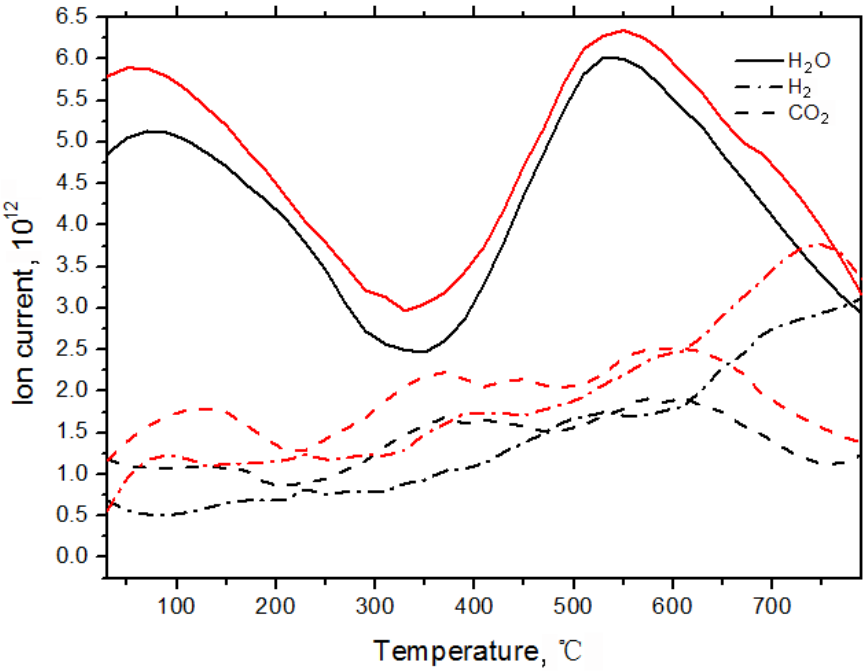

(b)

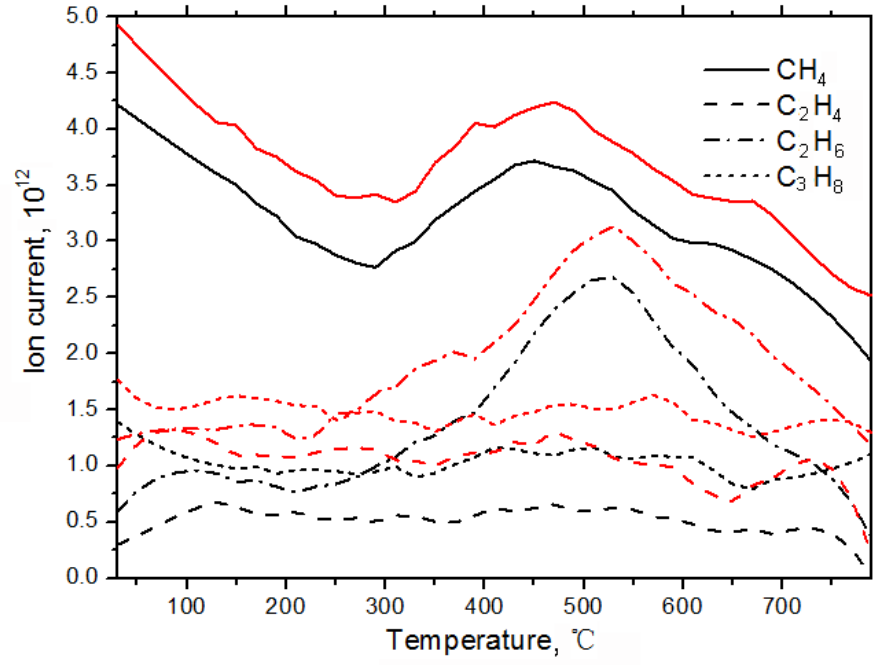

Fig. 2. Pyrolysis products of Bogda oil shale samples obtained at different temperatures: (a) CO_2, H_2, H_2O; (b) CH_4, C_2H_4, C_2H_6, C_3H_8.

3.2. Kinetic parameters

The pyrolysis of solids is usually modelled using the n-th order reaction kinetics model. Based on this model, the following kinetic equation for the pyrolysis of oil shale specimens was constructed to solve the pertinent kinetic parameters [17, 18]:

$$\frac{da}{dT} = \frac{A}{\beta}\exp[-e/RT]\cdot(1-a)^n . \tag{1}$$

The kinetic parameters are generally solved using the integral and differential methods. The Coast-Redfern integral method is the most popular approach for an approximate solution of kinetic parameters.

When $n = 1$,

$$\ln[\frac{-\ln(1-a)}{T^2}] = \ln[\frac{AR}{\beta E}(1-\frac{2RT}{E})] - \frac{E}{RT}, \tag{2}$$

where T is the temperature, K; β is the heating rate, K/min; R is the ideal gas constant, kJ $mol^{-1}\cdot K^{-1}$; A is the pre-exponential factor, min^{-1}; E is the activation energy, kJ mol^{-1}; a denotes the conversion percentage, %. According to the TG curve:

$$a = \frac{W_0 - W}{W_0 - W_f}, \tag{3}$$

where W_0 and W_f are the initial and final masses of the specimens, respectively, W is the mass of the unreacted specimens remaining at time t.

As seen from Table 2, the activation energy was 79.8–81.4 kJ/mol, and the heating rate exerted but a little influence on the activation energy or the pre-exponential factor. This phenomenon reflected the fact that the rupture of side chains with poor thermostability and active functional groups occurred first. As the reaction progressed, the rupture of carbon-carbon bonds in aromatic nuclei and the decomposition of long-chain alkanes began within the oil shale specimens. In Bogda oil shale, there were numerous side chains and active functional groups, which caused its low activation energy value, unlike oil shales from other areas.

Table 2. Pyrolysis kinetic parameters of Bogda oil shale at different heating rates

Heating rate, $K\cdot min^{-1}$	Temperature range, °C	Activation energy (E), $kJ\cdot mol^{-1}$	Correlation coefficient (R)
10	320–630	79.8	0.997
20	320–630	81.4	0.998
30	320–630	80.5	0.997

3.3. Infrared spectroscopy

As displayed in Figure 3 and Table 3, the absorption peaks at 2947 cm^{-1} ($\nu_s CH_2$) and 2842 cm^{-1} ($\nu_s CH_2$) belonged to the vibration of the functional

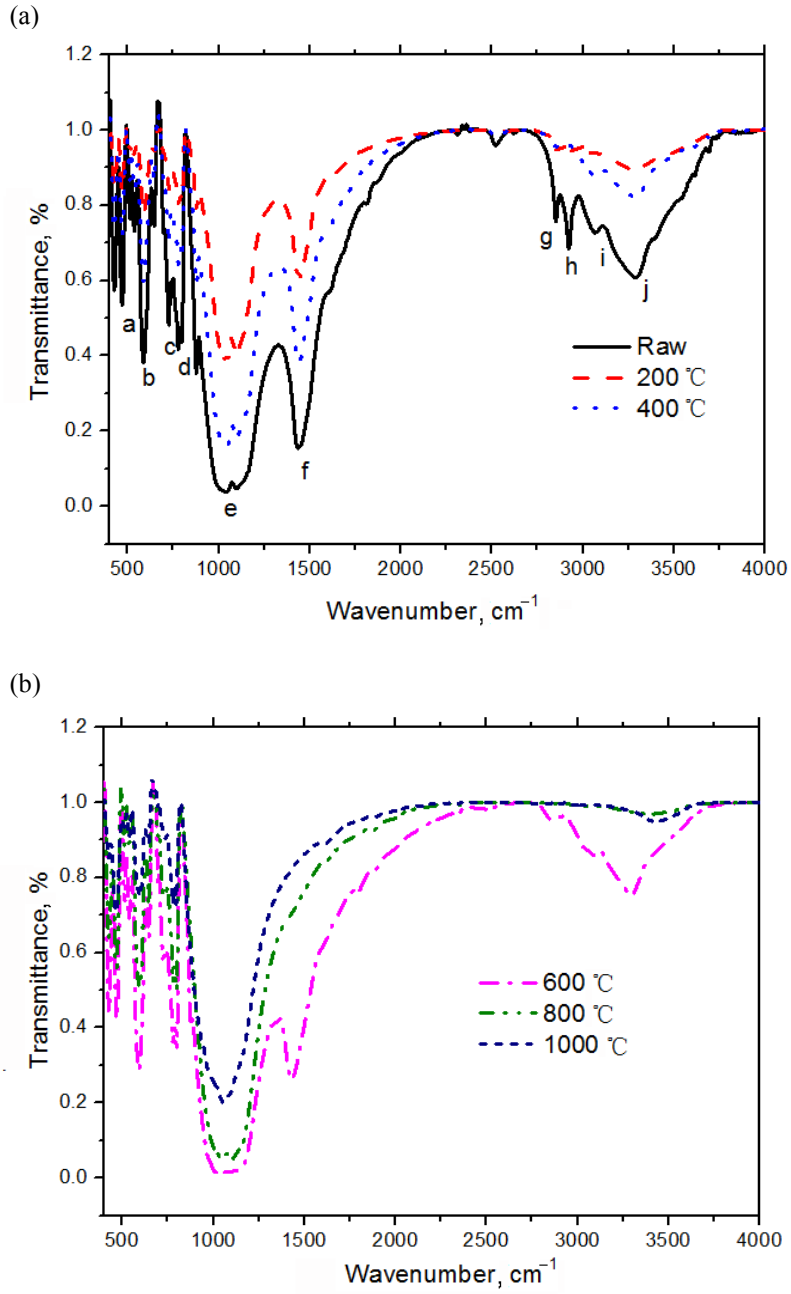

Fig. 3. IR spectra of Bogda oil shale samples at different temperatures: (a) low-temperature stage; (b) high-temperature stage.

Table 3. Band assignments for FTIR spectra of Bogda oil shale

Band No.	Wavenumber, cm^{-1}	Code	Absorption peak
1	567	a	C–H
2	718	b	C–H
3	787	c	Si–O–Si
4	857	d	Si–O–Si
5	1031–1135	e	C–O
6	1450	f	C=C
7	2842	g	C–H
8	2947	h	C–H
9	3086	i	C–H
10	3306	j	O–H

groups of aliphatic C–H bonds. The peak at 1450 cm^{-1} was attributed to the stretching vibration of the C=C skeleton of the aromatic ring. The peaks at 567 cm^{-1} and 718 cm^{-1} were assigned to the C–H vibration of the aromatic band, while that at 3306 cm^{-1} was the stretching vibration of the O–H group. This indicated that the oil shale specimens contained large amounts of organic functional groups, mainly including aliphatic and aromatic compounds [19, 20]. In the low-band fingerprint region, the adsorption peak of minerals was a major one, the stretching vibration peak of Si–O could be seen between 857 and 787 cm^{-1}, suggesting that the oil shale specimens contained abundant minerals. The intensity of the peaks of organic functional groups in the samples varied with temperature. As the pyrolysis temperature in the low-band region went up, the intensity of the adsorption peak of aliphatic C–H bonds decreased at temperatures above 200 °C, as seen in the 2947–2842 cm^{-1} region. While the intensity of the peaks decreased significantly with the temperature rising above 400 °C, the intensity of the peak of the C=C double bond diminished slowly and decreased significantly at temperatures higher than 800 °C. Furthermore, the adsorption peaks of the C–O functional groups and minerals increased at first and then tended to decrease. This indicated that with rising temperature there took place a series of complex reactions, including oxidation, hydrolysis, dehydrogenation and condensation, whose intensities were temperature-dependent. Figure 4 illustrates the variation of the content of functional groups in Bogda oil shale with increasing temperature. The C–O content in oil shale fluctuated across the range from room temperature to 1000 °C. In raw oil shale, the C–O content was approximately 250 a.u. and declined to 120 a.u. when the pyrolysis temperature rose to 400 °C. However, the C–O content increased significantly between 400 and 600 °C. This could be explained by the decomposition and generation of oxygen-containing groups in oil shale. In the initial stage of pyrolysis, the content of primary oxygen-containing functional groups decreased, while more new groups were produced when the temperature rose. In contrast, a slight decrease of C=C, –OH and $–CH_2–$ could be observed with the increase in

temperature, which suggested that these groups were gradually broken down during the pyrolysis process.

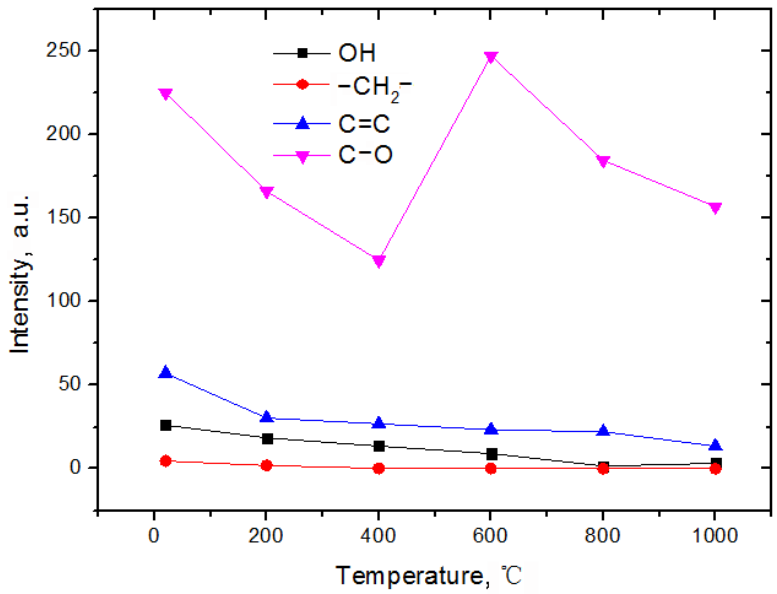

Fig. 4. Functional group contents of Bogda oil shale samples at different temperatures.

3.4. XRD

XRD results for Bogda oil shale are shown in Figure 5. The main minerals in oil shale were primarily clay minerals, quartz, micas, calcite, frondelite and pyrite [21]. Furthermore, small amounts of saline minerals and some trace minerals were also determined, with quartz being the most abundant. With increasing pyrolysis temperature, the 2θ of different peaks varied slightly in the XRD spectra of the residues of pyrolysed samples, while the intensity of the peaks decreased. These results demonstrated that most of the minerals underwent the decomposition reaction with increasing temperature, while organic carbon was found to undergo decomposition and condensation reactions. As the temperature increased, the crystal structure of the minerals in oil shale changed, causing a variation in 2θ and the peaks of quartz and micas. With the temperature increasing from 400 to 600 °C, the diffraction peaks of calcium carbonate declined and basically disappeared at 800 °C. At 1000 °C, the intensity of the peaks of most minerals, excluding quartz, largely weakened, revealing that the temperature exerted a significant effect on the mineral structure and composition of the oil shale specimens.

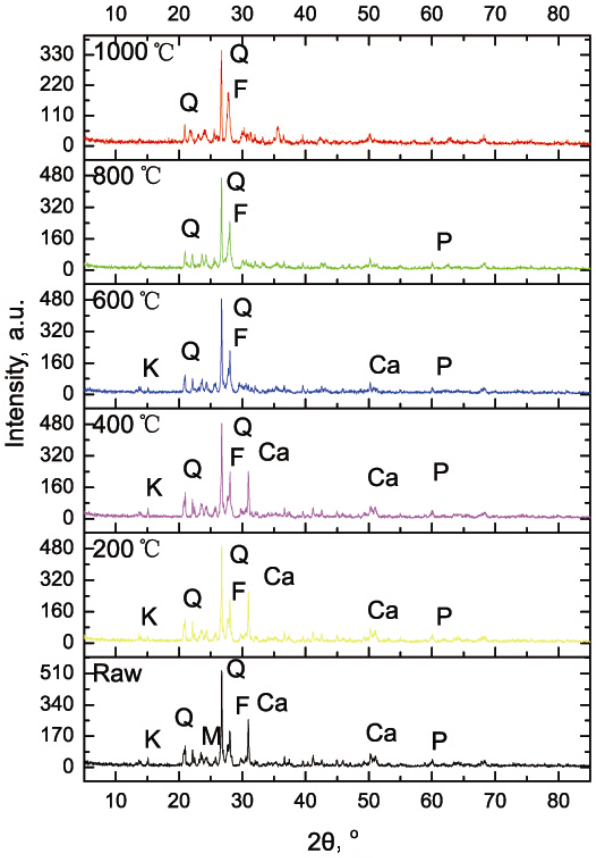

Fig. 5. XRD of Bogda oil shale samples at different temperatures.

3.5. SEM and EDS

SEM results for Bogda oil shale samples are shown in Figure 6. The microstructure of raw oil shale samples was evenly arranged. From a microscopic perspective, the porosity and permeability of Bogda oil shale are rather poorly developed. With the temperature increasing, the small-molecular organic substance was gradually emitted from oil shale. At 600 °C, some cracks and pores were formed in oil shale under the influence of heating. Moreover, some minerals even melted at higher temperatures (1000 °C). As seen from Figure 7, different elements such as C, K, Ca, Mg, Al, Fe, O and Si were found on the oil shale sample surface. However, when the temperature rose to 1000 °C, some elements were hard to be detected. These changes may be explained by the pyrolysis, vitrification and recrystallization of the minerals in oil shale. The said phenomena were in accord with the XRD results. In summary, the pyrolysis of Bogda oil shale was accompanied by complex mineral transformations and element migration.

(a)

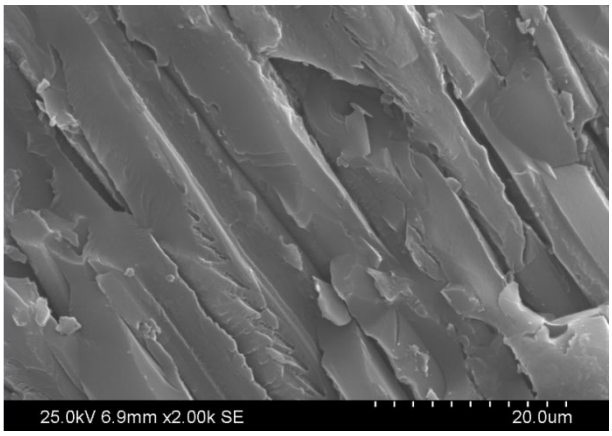

(b)

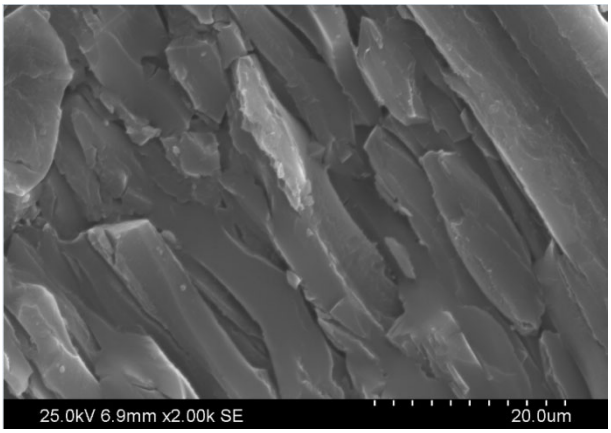

(c)

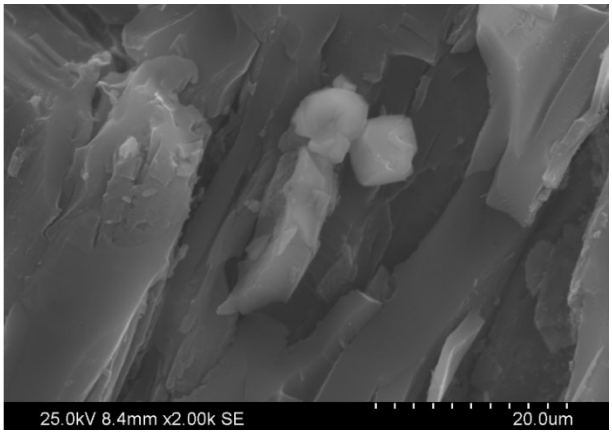

Fig. 6. SEM of Bogda oil shale samples at different temperatures: (a) raw sample; (b) sample at 600 °C; (c) sample at 1000 °C.

(a)

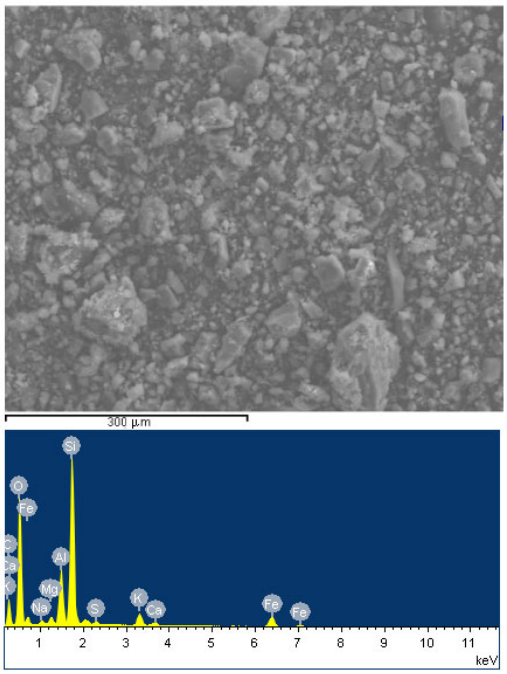
300 µm
Si
O
Fe
Al
Mg
Na
S
K
Ca
Fe
Fe
1 2 3 4 5 6 7 8 9 10 11
keV

(b)

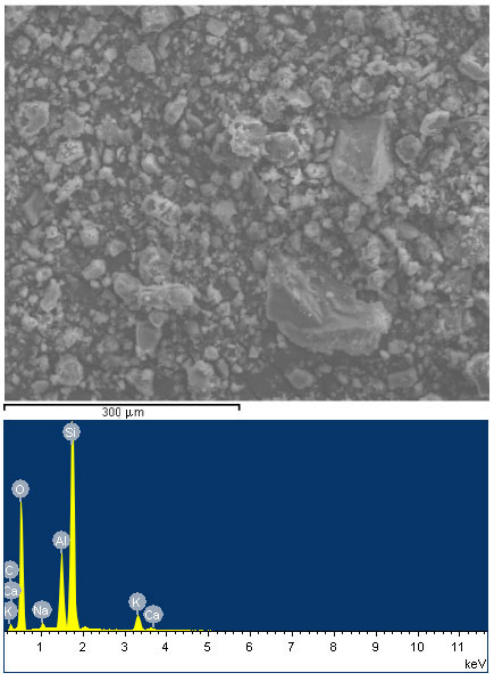
300 µm
Si
O
Al
Na
K
Ca
1 2 3 4 5 6 7 8 9 10 11
keV

(c)

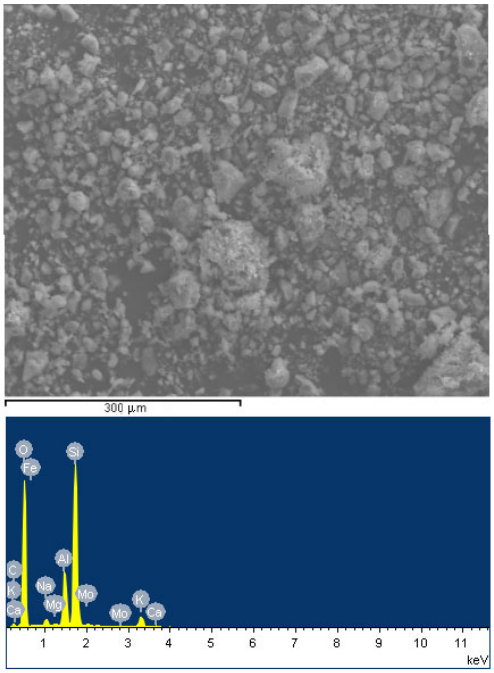

Fig. 7. EDS of Bogda oil shale samples at different temperatures: (a) raw sample; (b) sample at 600 °C; (c) sample at 1000 °C.

4. Conclusions

1. The pyrolysis of Bogda oil shale was conducted in the following three temperature ranges: room temperature–320 °C, 320–630 °C, and 630–800 °C. In the 320–630 °C range, the pyrolysis reaction was the most intensive, during which practically all the volatile matter was released. In the third temperature region, from 630 to 800 °C, the pyrolysis of carbonates took place.
2. Based on the Fourier transform infrared spectroscopy analysis, the oil shale samples primarily contained aliphatic and aromatic compounds, oxygen-containing functional groups, and silicate. As the temperature of pyrolysis increased, the $–CH_2–$ molecules were pyrolysed first. With increasing temperature, the pyrolysis of C=C occurred. Furthermore, the adsorption peaks of C–O and Si–O groups revealed changes to have taken place in their composition.
3. The structure and morphology of minerals in Bogda oil shale were complex. The minerals mainly included quartz, micas, kaolinite, calcite, frondelite and pyrite. With increasing temperature, the mineral structures and compositions of oil shale underwent significant changes, as reflected by the rapid pyrolysis of carbonates at temperatures higher than 600 °C.

Acknowledgements

This work was supported by the National Natural Science Foundation of China (Grant No. 51604182).

REFERENCES

1. Xu, S. C., Liu, Z. J., Zhang, P., Boak, J. M., Liu, R., Meng, Q. T. Characterization of depositional conditions for lacustrine oil shales in the Eocene Jijuntun Formation, Fushun Basin, NE China. *Int. J. Coal Geol.*, 2016, **167**, 10–30.
2. Chen, C., Wang, W., Sun, Y. et al. Influence of the heat transfer efficiency of oil shale in situ fragmentation. In: *Progress of Geo-Disaster Mitigation Technology in Asia* (Wang, F., Miyajima, M., Li, T., Shan, W., Fathani, T., eds). Springer, Berlin, Heidelberg, 2013, 577–583.
3. Xie, H. P., Li, X. C., Fang, Z. M., Wang, Y. F., Li, Q., Shi, L., Bai, B., Wei, N., Hou, Z. M. Carbon geological utilization and storage in China: current status and perspectives. *Acta Geotech.*, 2014, **9**(1), 7–27.
4. Hayta, U., Bozkurt, P. A., Canel, M. Co-pyrolysis of lignite-oil shale mixtures. In: *3rd International Congress on Energy Efficiency and Energy Related Materials* (Oral, A., Bahsi Oral, Z., eds). Springer International Publishing, 2017, 73–79.
5. Yang, Q., Qian, Y., Zhou, H., Yang, S. Conceptual design and techno-economic evaluation of efficient oil shale refinery processes ingratiated with oil and gas products upgradation. *Energ. Convers. Manage.*, 2016, **126**, 898–908.
6. Strizhakova, Y. A., Usova, T. V. Current trends in the pyrolysis of oil shale: A review. *Solid Fuel Chem.*, 2008, **42**(4), 197–201.
7. Wang, W., Li, S., Li, L., Ma, Y., Yue, C., He, J. Pyrolysis characteristics of a North Korean oil shale. *Petrol. Sci.*, 2014, **11**(3), 432–438.
8. Bai, F., Sun, Y., Liu, Y., Guo, M. Evaluation of the porous structure of Huadian oil shale during pyrolysis using multiple approaches. *Fuel*, 2017, **187**, 1–8.
9. Hu, Z., Ma, X., Li, L. The synergistic effect of co-pyrolysis of oil shale and microalgae to produce syngas. *J. Energy Inst.*, 2016, **89**(3), 447–455.
10. Bai, F., Sun, Y., Liu, Y., Li, Q., Guo, M. Thermal and kinetic characteristics of pyrolysis and combustion of three oil shales. *Energ. Convers. Manage.*, 2015, **97**, 374–381.
11. Al-Ayed, O. S., Al-Harahsheh, A., Khaleel, A. M., Al-Harahsheh, M. Oil shale pyrolysis in fixed-bed retort with different heating rates. *Oil Shale*, 2009, **26**(2), 139–147.
12. Sadiki, A., Kaminsky, W., Halim, H., Bekri, O. Fluidised bed pyrolysis of Moroccan oil shales using the hamburg pyrolysis process. *J. Anal. Appl. Pyrol.*, 2003, **70**(2), 427–435.
13. Yu, H., Jiang, X. Study of pyrolysis property of Huadian oil shale. *J. Fuel Chem. Technol.*, 2001, **29**(5), 450–453.
14. Li, S. Y., Yue, C. T. Study of pyrolysis kinetics of oil shale. *Fuel*, 2003, **82**(3), 337–342.
15. Allred, V. D. Shale oil developments: Kinetics of oil shale pyrolysis. *Chem. Eng. Prog. Symp. Ser.*, 1966, **62**(8), 55–60.

16. Nazzal, J. M. The influence of grain size on the products yield and shale oil composition from the pyrolysis of Sultani oil shale. *Energ. Convers. Manage.*, 2008, **49**(11), 3278–3286.
17. Yao, Z., Ma, X., Wang, Z., Chen, L. Characteristics of co-combustion and kinetic study on hydrochar with oil shale: A thermogravimetric analysis. *Appl. Therm. Eng.*, 2017, **110**, 1420–1427.
18. Hu, A., Yuan, Q., Zhang, X. Analysis of the pyrolysis characteristics of oil shales based on TG- FTIR method. *Science & Technology Information*, 2008, **29**, 45–47 (in Chinese with English abstract).
19. Han, X. X., Kulaots, I., Jiang, X. M., Suuberg, E. M. Review of oil shale semicoke and its combustion utilization. *Fuel*, 2014, **126**, 143–161.
20. Amer, M. W., Marshall, M., Fei, Y., Jackson, W. R., Gorbaty, M. L., Cassidy, P. J., Chaffee, A. L. The structure and reactivity of a low-sulfur lacustrine oil shale (Colorado U.S.A.) compared with those of a high-sulfur marine oil shale (Julia Creek, Queensland, Australia). *Fuel Process. Technol.*, 2015, **135**, 91–98.
21. Farouk, S., Ahmad, F., Mousa, D., Simmons, M. Sequence stratigraphic context and organic geochemistry of Palaeogene oil shales, Jordan. *Mar. Petrol. Geol.*, 2016, **77**, 1297–1308.

Presented by J. Schmidt
Received December 7, 2017